Homolytic Reactions of Ligated Boranes. Part 19.[1] Relationships Between Structure, Reactivity and Enantioselectivity for Hydrogen-atom Abstraction by Chiral Amine–Boryl Radicals

Hai-Shan Dang, Valérie Diart, Brian P. Roberts* and Derek A. Tocher
Christopher Ingold Laboratories, Department of Chemistry, University College London, 20 Gordon Street, London, UK WC1H 0AJ

The molecular structures of optically active quinuclidine–isopinocampheylborane and of the polycyclic amine–borane formed by cyclisation of *N*-nopylpyrrolidine–borane have been determined by X-ray crystallography. These and related amine–borane complexes have been used previously as polarity-reversal catalysts to bring about kinetic resolution of racemic esters and ketones. The key step in these resolutions is enantioselective H-atom abstraction from an α-C–H group in the carbonyl compound by the chiral amine–boryl radical derived from the catalyst. *Ab initio* and semi-empirical molecular orbital calculations have been carried out for representative transition states involved in H-atom transfer to amine–boryl radicals and the roles of dipole–dipole interactions, stereoelectronic effects and hydrogen-bonding have been investigated. The steric demands of a variety of amine–boryl radicals in H-atom transfer reactions have been assessed by determining the relative rates of abstraction from the α-C–H bonds in diethyl malonate and diethyl methylmalonate.

Amine–boryl radicals **1** abstract hydrogen atoms rapidly and regioselectively from an α-C–H group in a ketone or a carboxylic acid derivative [eqn. (1)].[1–5] When the ligating

$$\underset{\mathbf{1}}{\text{Amine}\rightarrow\dot{\text{B}}\text{HR}} + \text{R}^1\text{R}^2\text{C(H)–C(O)X} \longrightarrow \text{Amine}\rightarrow\text{BH}_2\text{R} + \text{R}^1\text{R}^2\dot{\text{C}}\text{–C(O)X} \quad (1)$$

amine or the *B*-alkyl group is chiral, the hydrogen-atom transfer can be enantioselective and this reaction has been used to bring about kinetic resolution of racemic carbonyl-containing substrates.[1,3,4]

In Part 18 of this series,[1] we described the use of kinetic resolution to determine the enantioselectivity constants† (*s*) for α-hydrogen abstraction from a variety of chiral carbonyl compounds by optically active amine–boryl radicals. The more reactive substrate enantiomer could generally be predicted by consideration of the steric interactions between the substituents attached to the boron atom and those attached to the α-carbon atom in the diastereoisomeric transition states. However, the enantioselectivities found were not large and it has become apparent that, because of the very small energetic differences involved, the relative stabilities of the transition states sometimes cannot be assessed reliably on the basis of steric effects alone and with the aid only of simple hand-held molecular models. In general terms, the transition state energies could be determined by a subtle interplay of steric, stereoelectronic and electrostatic interactions, together with the effects of hydrogen-bonding and Lewis acid–Lewis base association in appropriate systems.

In order to gain further insight into the factors which govern chiral discrimination in these reactions, we have determined the structures of two optically active amine–borane precursors of the radicals **1** using X-ray crystallography. We have also carried out EPR spectroscopic experiments to assess the steric requirements of selected amine–boryl radicals and have performed molecular orbital calculations for some representative transition states involved in hydrogen-atom transfer.

† The enantioselectivity constant *s* is equal to k_A/k_B, where k_A and k_B are the rate constants for abstraction from the more and from the less reactive enantiomers, respectively.

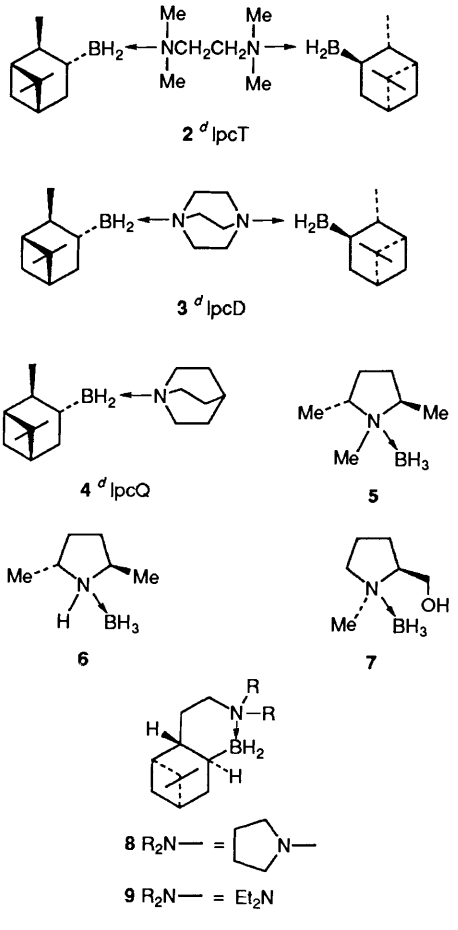

Results and Discussion

The preparations of the optically active amine–borane complexes **2–9** have been described previously.[1,6,7] The *N,N,N',N'*-tetramethylethylenediamine(TMEDA), 1,4-diazabicyclo[2.2.2]octane (DABCO) and quinuclidine complexes **2–4** with isopinocampheylborane ($IpcBH_2$) are those derived from (1*R*)-(+)-α-pinene by hydroboration; the superscript *d* or *l* is

Table 1 Enantioselectivity factors (s) obtained from kinetic resolutions of **10** and **11** in oxirane at −74 °C

	Catalyst							
Substrate	[d]IpcT **2**	[d]IpcD **3**	[d]IpcQ **4**	**5**	**6**	**7**	**8**	**9**
10[a]	6.7	3.0	3.2	1.4	1.3	2.0	1.8	2.1
11[b]	2.3	—	—	1.9	—	1.4	1.7	5.2

[a] The more reactive enantiomer is (4*S*,5*S*)-**10** with all catalysts. [b] The more reactive enantiomer is (3*R*)-**11** with all catalysts.

used with the acronyms shown to indicate whether the starting pinene was *dextro*- or *laevo*-rotatory.

Previously determined[1] enantioselectivity constants for α-hydrogen-atom abstraction from the racemic substrates **10** and **11** by the amine–boryl radicals derived from **2–9** are given in Table 1.

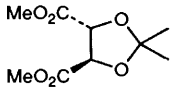

10

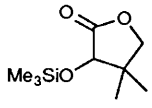

11

The amine–boryl radical derived from IpcT is appreciably more enantioselective in hydrogen-atom abstraction from **10** than is the corresponding radical derived from the DABCO complex IpcD. This suggests that the steric asymmetry * around boron in the transition state for abstraction by the former radical may be greater than that for abstraction by the latter. Alternatively, the second chiral borane residue in the amine–boryl radical from IpcT could interact in the transition state to increase enantioselectivity in a manner not possible for the more rigid DABCO complex. The single-crystal X-ray structure of [d]IpcT has been determined previously.[8] Although crystals suitable for X-ray diffraction could not be grown for IpcD, they could be obtained for the related monoborane complex IpcQ. The steric environment about boron in the transition states for abstraction by the amine–boryl radicals from IpcD and IpcQ should be very similar and, indeed, the same enantioselectivity is shown by both these radicals when they abstract from racemic **10** (see Table 1).

The crystal structure determined for [l]IpcQ is shown in Fig. 1. In Fig. 2(*a*) the mirror image of this (≡[d]IpcQ) is drawn for comparison with the structure of [d]IpcT [Fig. 2(*b*)] determined previously.[8] The geometry of the $IpcBH_2$ group is very similar in both complexes and is probably also similar in IpcD. Provided that the structures of these complexes in the solid state are close to those of the developing amine–boranes in the corresponding transition states **12** for H-atom transfer, molecular models indicate that the steric asymmetry around boron is greater for IpcT than for IpcD or IpcQ, suggesting that this is the likely reason for the greater chiral discrimination obtained with the TMEDA complex.

The polycyclic catalyst **8** is prepared by thermally induced cyclisation of the nopylamine–borane complex **13**.[1] The structure drawn for **8** assumes that *syn*-hydroboration has taken place from the less-hindered face of the double bond to give a *trans* ring junction. The X-ray crystal structure of **8** is shown in Fig. 3 and this confirms the assumptions made previously.[1] The relatively rigid structure of **8** makes this amine–borane, and related complexes with other *N*-alkyl groups, particularly suitable for probing the origins of the chiral discrimination

* The size difference between substituents of large, medium and small bulk.[1]

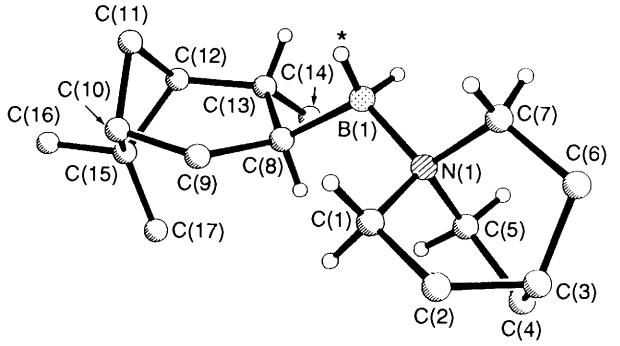

Fig. 1 Crystal structure of [l]IpcQ **4**; only key hydrogen atoms are shown. The hydrogen atom attached to boron and marked with an asterisk is that thought to be involved in H-atom transfer reactions (see the text). The BN and BC bond lengths are 1.636(6) and 1.620(7) Å, respectively, and the CBN angle is 115.9(4)°.

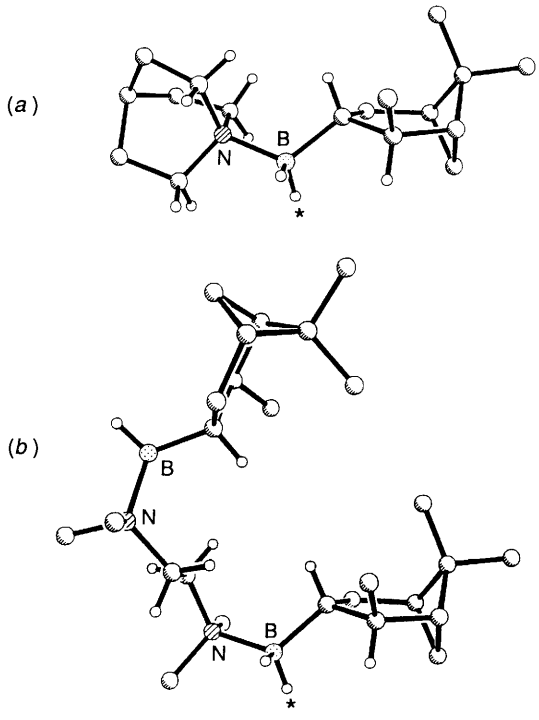

Fig. 2 (*a*) Mirror image of the crystal structure of [l]IpcQ (≡[d]IpcQ); (*b*) crystal structure of [d]IpcT **2**, drawn from the coordinates given by Soderquist *et al.* (ref. 8)

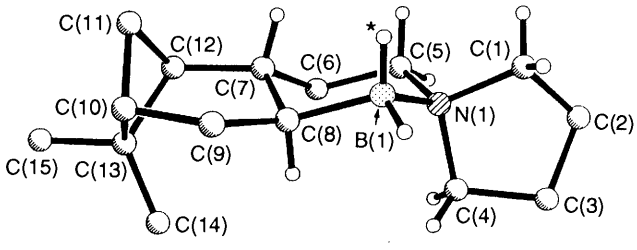

Fig. 3 Crystal structure of the polycyclic amine–borane **8**; only key hydrogen atoms are shown. The hydrogen atom attached to boron and marked with an asterisk is that thought to be involved in H-atom transfer reactions (see the text). The BN and BC bond lengths are 1.643(4) and 1.615(4) Å, respectively, and the CBN angle is 107.3(2)°.

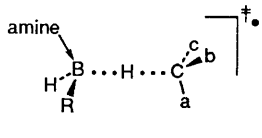

12

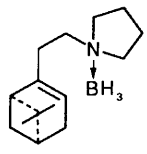

13

shown by the derived amine–boryl radicals. Of the two hydrogen atoms attached to boron in each of the complexes **2**, **4** and **8**, that which is the less sterically protected is indicated with an asterisk in Figs. 1–3. The hydrogen atom being transferred between carbon and boron in the preferred transition state of the type **12** will probably occupy a position similar to that of H*.

Electron Paramagnetic Resonance Studies.—In order to probe the steric demands of the amine–boryl radicals derived from **2**–**9**, the relative rates of α-hydrogen-atom abstraction from diethyl malonate **14** and diethyl methylmalonate **15** were measured using EPR spectroscopy under conditions of polarity-reversal catalysis.[9,10] Photolysis of di-*tert*-butyl peroxide (DTBP) produces the electrophilic *tert*-butoxyl radical which rapidly abstracts electron-rich hydrogen from boron in an amine–borane complex to give a nucleophilic amine–boryl radical, which in turn rapidly abstracts an electron-deficient α-hydrogen atom from the malonate [eqns. (2–4)]. The achiral

$$Bu^tO_2Bu^t \xrightarrow{h\nu} 2Bu^tO^\bullet \quad (2)$$

$$Bu^tO^\bullet + Amine{\rightarrow}BH_2R \longrightarrow Bu^tOH + Amine{\rightarrow}\dot{B}HR \quad (3)$$

$$Amine{\rightarrow}\dot{B}HR \xrightarrow[k_1]{H_2C(CO_2Et)_2\ \mathbf{14}} H\dot{C}(CO_2Et)_2\ \mathbf{16} \quad (4a)$$

$$Amine{\rightarrow}\dot{B}HR \xrightarrow[k_2]{H(Me)C(CO_2Et)_2\ \mathbf{15}} Me\dot{C}(CO_2Et)_2\ \mathbf{17} \quad (4b)$$

amine–boranes **18**–**21** were included for comparative purposes and the relative reactivities of these malonates towards the amine–boryl radical from trimethylamine–thexylborane† **22** has been determined previously in cyclopropane solvent.[2c]

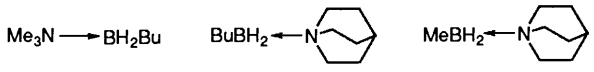

18

19

20

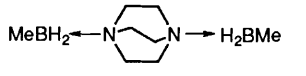

21

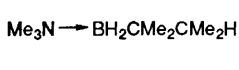

22

UV irradiation of an oxirane solution containing the amine–borane (0.15–0.30 mol dm^{-3}), the two malonates (each 0.2–1.0 mol dm^{-3}) and DTBP (15% v/v) afforded overlapping EPR spectra of the two radicals **16** and **17**, as described previously.[10]‡ The relative concentrations of **16** and **17** under steady-state conditions during continuous UV photolysis will be given by eqn. (5), provided that these two radicals are

$$k_1/k_2 = [\mathbf{15}][\mathbf{16}]/[\mathbf{14}][\mathbf{17}] \quad (5)$$

removed by self- and cross-reactions which have equal (diffusion-controlled) rate constants.[9,10] Values of k_1/k_2 at −84 °C were determined by double integration of appropriate non-overlapping lines in the EPR spectrum, usually for two different malonate concentration ratios [**14**]:[**15**]. Radical concentration ratios were confirmed by computer simulation of the spectra and the results are summarised in Table 2.

Only weak spectra of the radicals **16** and **17** were obtained when the secondary amine–borane **6** was used as polarity-reversal catalyst. We attribute this to the occurrence of a competitive reaction between the amine–boryl radical and its parent **6** to yield an electrophilic aminyl–borane radical incapable of abstracting hydrogen from the malonates.[11] The EPR spectrum of the aminyl–borane radical would consist of many lines and this radical would be difficult to detect in low concentration. When a solution of DTBP and **6** in *tert*-butyl alcohol–*tert*-pentyl alcohol (4:1 v/v) was UV irradiated at −6 °C, a complex spectrum which we assign to the expected aminyl–borane radical $Me\dot{C}H(CH_2)_2CH(Me)\dot{N}{\rightarrow}BH_3$ was observed [$a(3H_\beta)$ 48.2, $a(2H_\beta)$ 34.1, a(N) 17.2, $a(^{11}B)$ 11.2 and $a(^{10}B)$ 3.7(5) G].

For competitive hydrogen-atom abstraction by a series of amine–boryl radicals, polar effects in the transition states should be similar and the value of k_1/k_2 would be expected to increase with increasing steric congestion about the boron centre. The amine–boryl radicals from the complexes **18**–**20** of methyl- and butyl-boranes should be amongst the least sterically hindered and indeed give rise to the smallest values of k_1/k_2. The relatively large value of k_1/k_2 for abstraction catalysed by the DABCO complex of methylborane **21** is somewhat surprising. Similar selectivities are found for abstraction by the amine–boryl radicals derived from **5** and **7**–**9**, with diethyl malonate being about twice as reactive as diethyl methylmalonate. The isopinocampheylborane complexes are associated with much larger values of k_1/k_2, indicating increased steric hinderance around the boron centres in the derived amine–boryl radicals. Similar values of k_1/k_2 (9–10) are shown by the amine–boryl radicals from the quinuclidine and DABCO complexes, but an appreciably larger value (19) was obtained with the TMEDA complex as catalyst. This high chemoselectivity, which is presumably steric in origin, is probably related to the higher enantioselectivities obtained with IpcT in comparison with IpcD and IpcQ (see Table 1). The selectivity obtained with IpcT is similar to that found previously[2c] with $Me_3N{\rightarrow}BH_2Thx$, when a bulky tertiary alkyl group is attached to the boron centre in the amine–boryl radical which brings about hydrogen abstraction.

Molecular Orbital Calculations.—Calculations were carried out at *ab initio* and semiempirical levels for representative transition states involved in hydrogen-atom abstractions of the general type shown in eqn. (1). The GAUSSIAN 90 system of programs[12] was used for the *ab initio* work and the AM1 method,[13] implemented in version 6.0 of MOPAC,[14] was used for the semiempirical calculations.

The geometry of the transition state for the model reaction (6) was fully optimised at the UHF/4-31G* level[15] and the

$$H_3N{\rightarrow}\dot{B}H_2 + CH_3CHO \longrightarrow H_3N{\rightarrow}BH_3 + {}^\bullet CH_2CHO \quad (6)$$

resulting structure is shown in **23a** (see Fig. 4). Selected calculated parameters are given in Table 3. The single imaginary vibrational frequency (−1766 cm^{-1}) calculated for **23a** is associated with transfer of a hydrogen atom from the α-carbon atom to boron and the arrangement of these three atoms in the transition state is fairly close to linear ($\angle B\cdots H\cdots C$ = 159.9°). The C=O and $H_3N{\rightarrow}BH_2$ group dipoles are opposed in **23a** (φ = 59.0°, see structure **24**), resulting in a relatively small total dipole moment (μ = 2.64 D), and the presence of hydrogen-bonding between one NH group and the carbonyl-oxygen atom is indicated by the short NH···OC distance

† The 1,1,2-trimethylpropyl group is known as the thexyl group (Thx).
‡ The EPR parameters under these reaction conditions are: for **16**, $a(H_\alpha)$ 20.30, $a(4H_\delta)$ 1.40 G and g 2.0040, and for **17**, $a(3H_\beta)$ 23.92, $a(4H_\delta)$ 1.10 G and g 2.0037.

Table 2 Relative rate constants for hydrogen-atom abstraction by amine–boryl radicals from $H_2C(CO_2Et)_2$ and $MeCH(CO_2Et)_2$ in oxirane at −84 °C under conditions of polarity-reversal catalysis

	Amine–borane catalyst											
	18	**19**	**20**	**8**	**7**	**21**	**9**	**5**	**4** IpcQ	**3** IpcD	**2** IpcT	**22**[a]
k_1/k_2[b]	0.88	0.88	0.89	1.6	1.7	2.0	2.0	2.3	8.9	9.6	19	21

[a] In cyclopropane solvent; data from ref. 2(*c*). [b] Estimated error ± 5%.

Table 3 Selected calculated parameters for the transition states **23a** and **23b**

Structure (basis set)	Energy/ hartree	$\langle S^2 \rangle$	μ/D	$\tilde{\nu}_i$[a]/cm^{-1}	Interatomic distance/Å						Angle/°	
					NB	CC	CO	B···H	C···H	NH···O	∠B···H···C	φ[b]
23a (4-31G*)	−234.644 998	0.794	2.64	−1766.2	1.639	1.454	1.208	1.545	1.363	1.986	159.9	59.0
23b (3-21G)	−233.580 142	0.833	2.67	−1632.9	1.663	1.445	1.243	1.558	1.358	1.794	157.3	58.5

[a] Single imaginary vibrational mode characterising a transition state. [b] Defined in structure **24**.

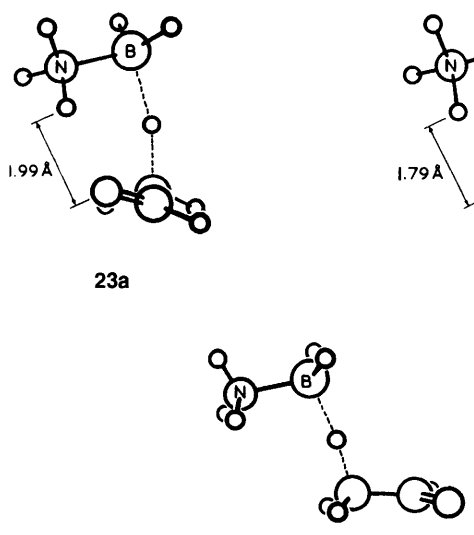

Fig. 4 Transition states for hydrogen-atom abstraction from acetaldehyde by the ammonia–boryl radical; **23a** at the 4-31G* level, **23b** and **c** at the 3-21G level

(r_{HO} = 1.99 Å). A very similar transition-state geometry (structure **23b**) was obtained using the smaller 3-21G basis set[15] and the effect of fixing the dihedral angle φ, while optimising all the other geometrical parameters, was investigated at this level. The dependences of the total energy (E) and the dipole moment

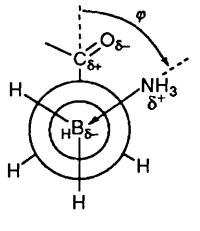

24

on φ are shown graphically in Fig. 5. As φ decreases from 180° towards its optimum value of 58.5° at this level, E decreases slowly at first and then more rapidly after r_{HO} becomes small enough for hydrogen-bonding to become energetically significant. Over this range of φ, the total dipole moment of the transition state decreases from 8.9 to 2.7 D and before the onset of hydrogen-bonding the decrease in total energy may be attributed to the stabilising intramolecular interaction between the C=O and $H_3N{\rightarrow}BH_2$ group dipoles, which increases as φ decreases.

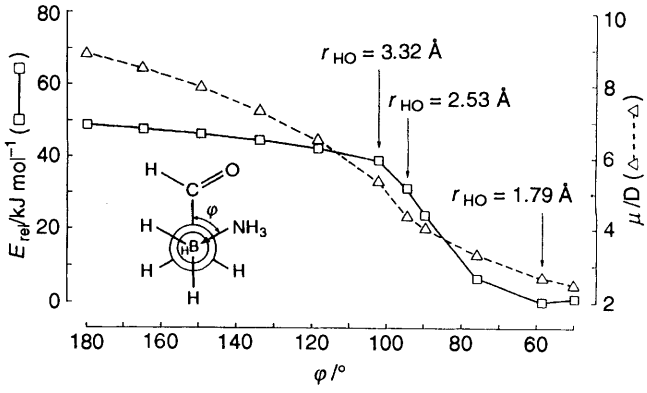

Fig. 5 Variation of the total energy and dipole moment for the transition state for hydrogen-atom abstraction from acetaldehyde by the ammonia–boryl radical, as a function of the dihedral angle φ, at the 3-21G level

When φ is between 180° and *ca.* 100°, the CHO plane is close to perpendicular to the H···C_α–C plane (see structure **23c** for which φ is 180°).* This is the stereoelectronically favoured arrangement which allows maximum delocalisation of negative charge from boron onto the carbonyl group, as represented by inclusion of structure **25** in a valence-bond description of the

$$[H_3\overset{+}{N}{-}BH_2\ H^{\cdot}\ H_2C{=}C(\bar{O})H] \quad \mathbf{25}$$

transition state. This arrangement also permits maximum delocalisation of the unpaired electron onto oxygen in the developing formylmethyl (vinyloxyl) radical. The importance of stabilising hydrogen-bonding in the transition state is further indicated by the tipping of the CHO plane, in the direction so as to reduce r_{HO}, which becomes increasingly pronounced for values of φ < *ca.* 100° (compare structures **23a** and **b** with **23c**).

* When φ falls between 180° and *ca.* 100°, and hydrogen-bonding is not possible, the value of ∠B···H···C is 173–170°, closer to linear than when hydrogen-bonding is present.

The ethyl radical is the isoelectronic organic analogue of the ammonia–boryl radical. For comparison, calculations were performed at the 4-31G* level for the transition state involved in hydrogen-atom abstraction from acetaldehyde by $H_3C\dot{C}H_2$, which is much less nucleophilic than $H_3N{\rightarrow}\dot{B}H_2$. Very shallow minima were located corresponding to the staggered conformations **26a** and **26b** (see Fig. 6) for which the values of φ† were 62.9° and 178.2°, respectively, although the energy of the transition state did not vary appreciably with φ. Steric interactions are unimportant because of the long C···H···C distance. The general features of **26a** are similar to those of the BN analogue **23a**, except for the absence of intramolecular hydrogen-bonding (and of the consequent tipping of the formyl group) in the former. Because of this lack of hydrogen-bonding and the much larger dipole–dipole interactions present for the BN analogue, the conformation **26b** is less stable than **26a** by only 0.9 kJ mol^{-1} (**23c** is less stable than **23b** by 48.5 kJ mol^{-1}). In both **26a** and **26b** the C···H···C grouping is close to linear (176.4° and 175.8°, respectively).

The charge on the CH_3CHO fragment in **26a** is small and negative (−0.005), in accord with the weakly nucleophilic nature of the ethyl radical. The charge on the oxygen atom is −0.476. In contrast, in **23a** the charge on the CH_3CHO residue is much more negative (−0.232 with, of course, an equal positive charge on the $H_3N{\rightarrow}BH_2$ residue) and the charge on oxygen is significantly increased to −0.572. This large degree of charge transfer from $H_3N{\rightarrow}\dot{B}H_2$ to the aldehyde in the transition state accords with the highly nucleophilic character of the amine–boryl radical, as represented in valence bond terms by a large contribution from canonical structure **25**.

We conclude that the optimum transition state geometry for reaction (6) is influenced by (i) stereoelectronic factors, (ii) the electrostatic interaction between the C=O and $H_3N{\rightarrow}BH_2$ group dipoles, and (iii) the existence of hydrogen-bonding between one NH group and the carbonyl-oxygen atom. Of course, the calculations refer to isolated species in the gas phase and do not take account of possible solvent effects, which might be important for such polar transition states.

Stabilising hydrogen-bonding of the type present in the transition state for reaction (6) is possible for reactions of the amine–boryl radical derived from the secondary amine–borane **6**, but not for tertiary amine–boryl radicals which lack an NH group. The chiral discrimination achieved in hydrogen-atom abstraction from **10** catalysed by **5** is essentially unchanged when **6** is the catalyst and thus, if hydrogen-bonding is important in the transition state, it does not have any significant influence on the enantioselectivity in this instance. An important limitation when attempting to use primary or secondary amine–boranes as polarity-reversal catalysts is the rapidity with which the derived amine–boryl radicals can be converted into electrophilic aminyl–borane radicals by abstracting hydrogen from an NH group in their parent[11] (*cf.* above).

Steric interactions between the reactants will also become important when the substituents are sufficiently bulky and 'front strain' in a crowded transition state could become the dominant factor in determining the activation energy for hydrogen-atom transfer. For bulky reactants, the more reactive enantiomer of the substrate does appear to be predictable solely by consideration of the steric chiralities[3] of the substrate- and amine–borane-derived moieties in the transition state.[1,3] Attempts to determine transition states for more complex reactants using the AM1 semiempirical method with full geometry optimisation were unsuccessful, possibly due to problems with the parametrisation for boron, because hydrogen-atom transfer was predicted to occur with a negligible energy barrier. This difficulty was circumvented by fixing the B···H and H···C_α bond lengths at the 4-31G*-optimised values for **23a** (1.545 and 1.363 Å, respectively) and minimising the total energy with respect to all other geometrical parameters. The transition states for reactions (7) and (8),

$$Me_3N{\rightarrow}\dot{B}H_2 + CH_3CHO \longrightarrow Me_3N{\rightarrow}BH_3 + {}^{\bullet}CH_2CHO \quad (7)$$

$$Me_3N{\rightarrow}\dot{B}H_2 + CH_3CO_2Me \longrightarrow Me_3N{\rightarrow}BH_3 + {}^{\bullet}CH_2CO_2Me \quad (8)$$

obtained in this fashion, are shown in structures **27** and **28**, respectively (see Fig. 7). Repulsive steric interactions between substrate and amine–boryl residues are still relatively unimportant in determining transition state geometries for these reactions, because of the long B···H···C_α distance. The conformations about the near-linear B···H···C groupings are similar to those in **23a** and **23b**, with the dihedral angle φ equal to 48.1° for **27** and 62.2° for **28**, although the carbonyl plane is now close to perpendicular to the H···C_α-C plane in both structures. Hydrogen-bonding is now not possible, but the drive to oppose the C=O and $H_3N{\rightarrow}BH_2$ group dipoles remains.

Interaction between a substrate-carbonyl group and the pendant OH group in the amine–boryl radical **29** derived from **7**, might be important in determining the relative energies of diastereoisomeric transition states and some circumstantial evidence has been found for such an effect.[1] AM1 calculations on the transition state for hydrogen-atom abstraction from methyl acetate by **29** predicted the structure **30** (see Fig. 8), which does indicate the presence of OH···O=C hydrogen-bonding.

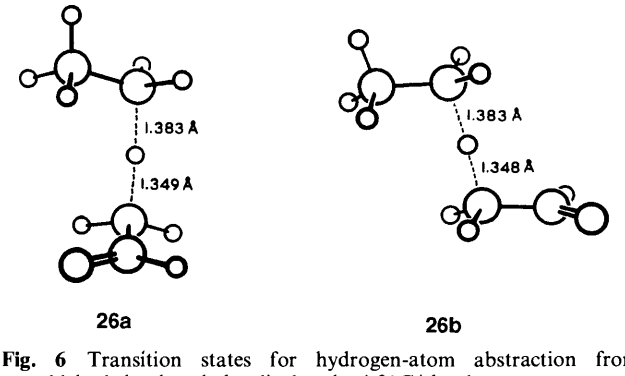

Fig. 6 Transition states for hydrogen-atom abstraction from acetaldehyde by the ethyl radical at the 4-31G* level

† Here φ refers to the CCCC dihedral angle defined in the same way as for the isoelectronic BN system in **24**.

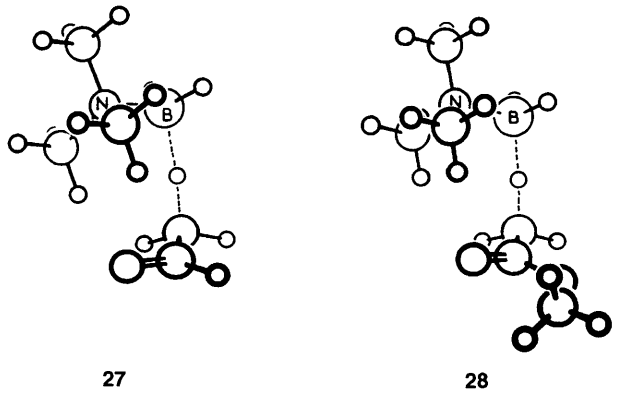

Fig. 7 Transition states for hydrogen-atom abstraction from acetaldehyde (**27**) and from methyl acetate (**28**) by the trimethylamine–boryl radical, obtained using the AM1 method

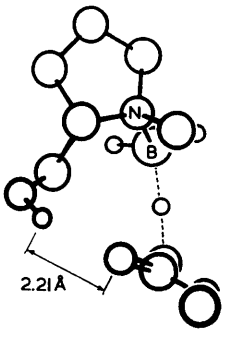

30

Fig. 8 Transition state for hydrogen-atom abstraction from methyl acetate by the amine–boryl radical **29**, obtained using the AM1 method

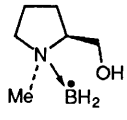

29

Calculations were also performed on the transition state for hydrogen-atom transfer from methyl acetate to the amine–boryl radical derived from the polycyclic complex **8**; as before, the B • • • H and C • • • H distances were fixed at 1.545 and 1.363 Å, respectively. The transition state was more stable by 7.5 kJ mol^{-1} when the B • • • H bond was axial than when it was equatorial, in agreement with our previous qualitative prediction based on examination of molecular models (see above and Fig. 3),[1] and this preference for axial hydrogen-atom transfer should increase with more bulky substrates.

Experimental

Materials.—NMR spectra were recorded using a Varian VXR-400 instrument (400 MHz for ^1H). The solvent was $CDCl_3$ and chemical shifts are reported relative to Me_4Si (^1H and ^{13}C) and to external $Et_2O{\rightarrow}BF_3$ (^{11}B); *J*-values are quoted in Hz. The preparations of the amine–borane complexes **2–9** have been described previously.[1,2,6,7] Trimethylamine–butylborane **18** was prepared by the method of Hawthorne.[10,16] Di-*tert*-butyl peroxide (98%, Aldrich) was passed down a column of basic alumina (activity 1) and distilled (b.p. 46–47 °C/76 Torr) and oxirane (Fluka) was used as received.

Quinuclidine–Butylborane **19**.—A solution of trimethylamine–butylborane (2.36 g, 18.3 mmol) and quinuclidine (1.89 g, 17.0 mmol) in benzene (10 cm^3) was heated under reflux for 4 h under argon. The solvent was removed by evaporation under reduced pressure and the residual oil was distilled to give **19** (2.77 g, 90%), b.p. 97–100 °C/0.03 Torr (Found: C, 73.0; H, 13.2; N, 7.8. $C_{11}H_{24}BN$ requires C, 72.9; H, 13.4; N, 7.7%); δ_H 0.31 (m, 2 H), 0.88 (t, 3 H, *J* 7.27), 1.18 (m, 2 H), 1.29 (m, 2 H), 1.73 (m, 6 H), 1.99 (sept, 1 H, *J* 3.23) and 2.96 (m, 6 H) (the BH_2 resonance was obscured); δ_C 14.33, 20.98, 25.30, 26.80, 31.70, 51.90 and 52.10 (the peak from the carbon attached to boron was too broad to detect); δ_B −1.69 (br t, J_{BH} 89).

Quinuclidine–Methylborane **20**.—This was prepared in the same way as **19** from trimethylamine–methylborane,[10] b.p. 66–68 °C/0.03 Torr (Found: C, 69.1; H, 13.2; N, 10.2. $C_8H_{18}BN$ requires C, 69.1; H, 13.1; N, 10.1%); δ_H −0.23 (t, 3 H, *J* 5.79), 1.59 (br q, 2 H, *J ca.* 93), 1.67 (m, 6 H), 1.97 (sept, 1 H, *J* 3.23) and 2.87 (m, 6 H); δ_C 20.69, 24.90 and 51.18 (the peak from the carbon attached to boron was too broad to detect); δ_B −8.33 (br t, *J ca.* 93).

DABCO–Bis(methylborane) **21**.—This was prepared in a similar way to **19** from trimethylamine–methylborane (1.83 g, 21.0 mmol) and DABCO (1.07 g, 9.5 mmol) in benzene (10 cm^3). After heating under reflux for 4 h the solution was allowed to cool to room temperature when some of the product crystallised. Hexane (5 cm^3) was added and the mixture was kept at 5 °C overnight. The amine–borane was removed by filtration and dried under reduced pressure (0.05 Torr) for 4 h at room temperature to give **21** (1.46 g, 92%), m.p. 167–178 °C (decomp.) (Found: C, 57.5; H, 13.2; N, 16.7. $C_8H_{22}B_2N_2$ requires C, 57.2; H, 13.2; N, 16.7%); δ_H −0.20 (t, 6 H, *J* 5.86), 1.81 (br q, 4 H, *J ca.* 98) and 3.30 (s, 12 H); δ_C 49.16 (the peak from the carbon attached to boron was too broad to detect); δ_B −7.10 (br t, *J ca.* 99).

No changes were observed in the NMR spectra of the complexes **19–21** after they had been kept exposed to the atmosphere for 1 week. The complex **19** shows particular promise as a readily prepared and easily handled amine–alkylborane for the generation of alkyl radicals from chloroalkanes at low temperatures for EPR studies[2e] and as an achiral polarity-reversal catalyst.[2]

EPR Spectroscopy.—EPR spectra were recorded during continuous UV irradiation of samples positioned in a standard variable temperature insert in the microwave cavity of a Varian E-109 or Bruker ESP-300 spectrometer operating at 9.1–9.4 GHz. The light source was a 500 W mercury discharge lamp (Osram HBO 500 W/2) and the optical system has been described previously.[10] Samples were prepared using a vacuum line and were sealed in evacuated Suprasil quartz tubes (2 mm i.d., 0.5 mm wall). Stock mixtures of diethyl malonate and diethyl methylmalonate (both distilled before use) were made up by weight and portions of these were used for sample preparation. The experimental methods for determination of relative rate constants using the EPR method have been described in detail previously.[10]

X-Ray Crystallography.—Data were collected on a Nicolet R3mV diffractometer at 20 °C using graphite monochromated Mo-Kα radiation. Three standard reflections monitored throughout the data collection showed no loss in intensity with time. The data were corrected for Lorentz and polarisation effects. The structures were solved by direct methods and developed using alternating cycles of least squares refinement and difference-fourier synthesis. Non-hydrogen atoms were refined anisotropically while hydrogens were placed in idealised positions and assigned a common isotropic thermal parameter (U = 0.08 $Å^2$). All calculations were performed with the SHELXTL PLUS program package[17] on a MicroVax II computer. Atomic coordinates, bond lengths and angles and thermal parameters have been deposited with the Cambridge Crystallographic Data Centre (see 'Instructions for Authors,' *J. Chem. Soc., Perkin Trans. 2,* 1994, issue 1).

Crystal data for ^{t}IpcQ **4**. $C_{17}H_{32}B_1N_1$, M = 261.3. Orthorhombic, space group $P2_12_12_1$, a = 9.279(3), b = 9.596(3), c = 19.250(5), U = 1714 $Å^3$ (by least-squares refinement of diffractometer angles for 35 reflections in the range 12° ≤ 2θ ≤ 22°, λ = 0.710 73 Å), Z = 4, F(000) = 584, D_c = 1.01 g cm^{-3}, μ(Mo-Kα) = 0.53 cm^{-1}. Colourless block 0.65 × 0.60 × 0.45 mm. Full-matrix least-squares refinement of 172 parameters gave R = 0.0605 (R_w = 0.0639) for 1425 independent reflections [$I \geq 3\sigma(I)$] in the range 5° ≤ 2θ ≤ 55°. The final electron density difference map was featureless with the largest peak 0.21 e $Å^{-3}$.

Crystal data for the amine–borane complex **8**. $C_{15}H_{28}B_1N_1$, M = 233.25. Orthorhombic, space group $P2_12_12_1$, a = 7.006(3), b = 7.876(3), c = 26.811(11), U = 1479 $Å^3$ (by least-

squares refinement of diffractometer angles for 30 reflections in the range $15° \leq 2\theta \leq 27°$, $\lambda = 0.710\,73$ Å), $Z = 4$, $F(000) = 520$, $D_c = 1.05$ g cm^{-3}, μ(Mo-Kα) = 0.55 cm^{-1}. Colourless block 0.75 × 0.35 × 0.30 mm, prepared by slow sublimation in an evacuated sealed tube. Full-matrix least-squares refinement of 154 parameters gave $R = 0.0559$ ($R_w = 0.0637$) for 1985 independent reflections [$I \geq 3\sigma(I)$] in the range $5° \leq 2\theta \leq 50°$. The final electron density difference map was featureless with the largest peak 0.28 e Å^{-3}.

Acknowledgements

We thank the SERC for support.

References

1 Part 18, H.-S. Dang, V. Diart and B. P. Roberts, *J. Chem. Soc., Perkin Trans. 1*, 1994, issue 8.
2 (*a*) V. Paul and B. P. Roberts, *J. Chem. Soc., Chem. Commun.*, 1987, 1322; (*b*) V. Paul and B. P. Roberts, *J. Chem. Soc., Perkin Trans. 2*, 1988, 1183; (*c*) V. Paul, B. P. Roberts and C. R. Willis, *J. Chem. Soc., Perkin Trans. 2*, 1989, 1953; (*d*) H.-S. Dang and B. P. Roberts, *Tetrahedron Lett.*, 1992, **33**, 4621 (corrigendum p. 7070) and 6169; (*e*) P. Kaushal, P. L. H. Mok and B. P. Roberts, *J. Chem. Soc., Perkin Trans. 2*, 1990, 1663; (*f*) H.-S. Dang and B. P. Roberts, *J. Chem. Soc., Perkin Trans. 1*, 1993, 891.
3 P. L. H. Mok, B. P. Roberts and P. T. McKetty, *J. Chem. Soc., Perkin Trans. 2*, 1993, 665.
4 P. L. H. Mok and B. P. Roberts, *J. Chem. Soc., Chem. Commun.*, 1991, 150.
5 P. L. H. Mok and B. P. Roberts, *Tetrahedron Lett.*, 1992, **33**, 7249.
6 (*a*) H. C. Brown, J. R. Schwier and B. Singaram, *J. Org. Chem.*, 1978, **43**, 4395; (*b*) B. Singaram and J. R. Schwier, *J. Organomet. Chem.*, 1978, **156**, Cl; (*c*) H. C. Brown, B. Singaram and J. R. Schwier, *Inorg. Chem.*, 1979, **18**, 51; (*d*) A. K. Mandal, P. K. Jadhav and H. C. Brown, *J. Org. Chem.*, 1980, **45**, 3543.
7 P. K. Jadhav and M. C. Desai, *Heterocycles*, 1982, **18**, 233.
8 J. A. Soderquist, S.-J. Hwang-Lee and C. L. Barnes, *Tetrahedron Lett.*, 1988, **29**, 3385.
9 A. G. Davies, D. Griller and B. P. Roberts, *J. Chem. Soc. B*, 1971, 1823.
10 V. Diart and B. P. Roberts, *J. Chem. Soc., Perkin Trans. 2*, 1992, 1761.
11 I. G. Green and B. P. Roberts, *J. Chem. Soc., Perkin Trans. 2*, 1986, 1597; J. N. Kirwan and B. P. Roberts, *J. Chem. Soc., Perkin Trans. 2*, 1989, 539.
12 GAUSSIAN 90, Revision I, M. J. Frisch, M. Head-Gordon, G. W. Trucks, J. B. Foresman, H. B. Schlegel, K. Raghavachari, M. Robb, J. S. Binkley, C. Gonzalez, G. J. Defrees, D. J. Fox, R. A. Whiteside, R. Seeger, C. F. Melius, J. Baker, R. L. Martin, L. R. Kahn, J. J. P. Stewart, S. Topiol and J. A. Pople, Gaussian Inc., Pittsburgh PA, 1990.
13 M. J. S. Dewar, E. G. Zoebisch, E. F. Healy and J. J. P. Stewart, *J. Am. Chem. Soc.*, 1985, **107**, 3902.
14 MOPAC version 6.0; J. J. P. Stewart, *QCPE*, program no. 455.
15 W. J. Hehre, L. Radom, P. von R. Schleyer and J. A. Pople, *Ab Initio Molecular Orbital Theory*, Wiley, New York, 1986.
16 M. F. Hawthorne, *J. Am. Chem. Soc.*, 1961, **83**, 831.
17 G. M. Sheldrick, SHELXTL PLUS, an integrated system for refining and displaying crystal structures from diffraction data, University of Gottingen, 1986.

Paper 3/06897H
Received 18*th November* 1993
Accepted 7*th January* 1994